Nanoscale

PAPER

View Article Online
View Journal | View Issue



Cite this: *Nanoscale*, 2019, **11**, 17401

# A highly selective "turn-on" electroanalysis strategy with reduced copper metal–organic frameworks for sensing histamine and histidine†

Yue Hua, Yuanyuan Cai, Huan Liu, Yuqi Wan, Xiju Ding, Shuai Li and Hua Wang *

Received 5th July 2019,
Accepted 3rd September 2019

DOI: 10.1039/c9nr05681e

rsc.li/nanoscale

A highly selective and sensitive electroanalysis strategy has been developed for sensing histamine (HTA) and histidine (His) with "turn-on" signal outputs using copper nanocomposites (Cu NCs) of reduced copper metal–organic frameworks (Cu MOFs). It was discovered that the Cu NC-modified electrodes could display the sharp and stable oxidation peaks of solid-state CuCl electrochemistry at a low potential (about −0.10 V). More interestingly, once HTA or His was introduced, the peaking currents of the electrodes would increase due to the specific interaction between $Cu^{2+}$ and imidazole groups of HTA or His. A highly selective electroanalysis method was thereby developed for the detection of both HTA and His in the concentration range of 0.010–100 μM. Besides, the application feasibility of the developed electroanalysis strategy was demonstrated for the evaluation of HTA and His separately in red wine and urine samples. Such an electroanalysis candidate for HTA and His holds great potential for wide applications in the fields of food analysis and clinical disease diagnosis.

## Introduction

Nitrogenous biogenic amines, such as histamine (HTA), spermine, tryptamine, tyramine, putrescine, cadaverine, phenylethylamine, and spermidine, which are derived from the decarboxylase-catalyzed decarboxylation reactions of corresponding amino acids, may be present in a variety of food products such as beer, red wine, milk, and fish.[1,2] In particular, HTA as a metabolite of histidine (His) has been recognized to be responsible for the frequent outbreaks of food poisoning issues most known as scombroid poisoning,[2–5] as HTA with too high levels in the human body can lead to headache, hypertension, and poisoning, and even threaten human lives.[6–8] Therefore, HTA detection is of great interest in the food industry.[9] Moreover, His plays vital roles in many biological systems, such as the control of transportation of some metal ions such as $Cu^{2+}$ ions[10–12] and as a neurotransmitter in the central nervous system.[13] The analysis of His in human body fluids such as urine is of clinical importance for monitoring human health and diagnosis of some diseases such as "histidinemia" and metabolic disorders.[14–16]

To date, a variety of analytical techniques have been applied for probing HTA, typically high-performance liquid chromatography,[17–19] mass spectrometry,[5,20] capillary electrophoresis,[21] spectrophotometry,[22] colorimetry,[23] and fluorimetric methods.[24] Most of these methods, however, may suffer from some disadvantages such as expensive facilities, tedious operation, and complicated sample pre-treatment.[25] Alternatively, electrochemical detection technologies, which can present high detection sensitivity, easy operation, and portable devices suitable for on-site applications,[26,27] have been applied for the detection of HTA.[28–31] For example, Dong *et al.* described an electrochemical strategy for sensing HTA using Prussian blue–chitosan–gold nanocomposites.[28] Reddy and coworkers have designed a Cu@Pd-modified electrode for the determination of HTA.[29] Nevertheless, these current electroanalysis methods may involve complicated electrode modification and especially low analysis selectivity. In recent years, some efforts have been devoted to the development of solid-state electroanalysis strategies, which have been well recognized to be advantageous over the most conventional analysis strategies in terms of low redox potentials and high detection selectivity and/or sensitivity.[26,32,33] For example, Zhang *et al.* reported an electroanalysis method for DNA using solid-state $Ag^0$/AgCl electrochemistry.[32] A sensor has also been developed in our group for the sensitive detection of $Pb^{2+}$ ions by way of solid-state voltammetry of $PbCl_2$.[33] In addition, recent years have witnessed the rapid development of metal organic frameworks (MOFs) widely applied in the adsorption, separation,

*Institute of Medicine and Materials Applied Technologies, College of Chemistry and Chemical Engineering, Qufu Normal University, Qufu, 273165, P. R. China. E-mail: huawang@qfnu.edu.cn; Fax: +86 5374456306; Tel: +86 5374456306; http://wang.qfnu.edu.cn*

†Electronic supplementary information (ESI) available. See DOI: 10.1039/c9nr05681e

storage, catalysis, and sensing analysis fields.[34–36] As the most common representatives with high porosity, copper MOFs (Cu MOFs) have received special application interest, due to their merits of a uniform configuration, superior catalytic activity, and a large surface area.[37,38]

In the present work, Cu nanocomposites (Cu NCs) were initially synthesized by alternatively using $NaBH_4$ to reduce Cu MOFs for the electroanalysis of HTA and His. It was discovered that the electrodes modified with Cu NCs could display a sharp and stable oxidation peak at a low potential with solid-state CuCl electrochemistry. More importantly, once HTA or His was introduced, the peak currents would rationally increase due to the strong interaction between $Cu^{2+}$ and imidazole groups of HTA or His. A highly selective and sensitive "turn-on" electroanalysis strategy was thereby proposed for the evaluation of HTA and His separately in red wine and urine. To the best of our knowledge, this is the first report on the electroanalysis of HTA and His with the "turn-on" signal output based on solid-state CuCl electrochemistry at a desirably low potential using Cu NCs of $NaBH_4$-treated Cu MOFs.

## Experimental section

### Reagents

Copper nitrate ($Cu(NO_3)_2$) was purchased from Sinopharm Chemical Reagent Co. (China). Phosphate buffer saline (PBS) solution, glutathione (GSH), and 1,3,5-benzenetricarboxylic acid (BTC) were obtained from Aladdin Reagent Co., Ltd. (Shanghai, China). Nafion solution (5.0%), histidine (His), lysine (Lys), cysteine (Cys), tyrosine (Tyr), histamine (HTA), tyramine (Tym), and 1,4-butanediamine (DAB) were purchased from Sigma-Aldrich (Beijing, China). All other reagents were of analytical grade. Deionized water (>18 Mohm) was obtained from an ultrapure water system (Pall, USA). All glass containers were cleaned in turn with aqua regia and ultrapure water.

### Apparatus

Scanning electron microscopy (SEM, Sigma 500 VP, Germany) was utilized for the characterization of the prepared materials. Electrochemical measurements were conducted with an electrochemical workstation CHI 760D (CH Instrument, Shanghai, China) connected to a personal computer. A three electrode system was used consisting of a glassy electrode, a Pt wire counter electrode, and an Ag/AgCl reference electrode.

### Synthesis of Cu NCs

Cu MOFs were synthesized by a one-step solvothermal procedure using $Cu(NO_3)_2$ and a BTC ligand. Typically, an aliquot of 60 mL $Cu(NO_3)_2$ (3.6 mM) and 60 mL BTC (8.1 mM) both in ethanol were mixed by stirring for 10 min. The mixture of $Cu(NO_3)_2$ and BTC was then transferred into an autoclave, and the solvothermal reaction was carried out at 160 °C for 18 h. After it was cooled down to room temperature naturally, the reaction products were collected and centrifuged at 6000 rpm for 10 min to be further washed twice using ethanol. The above centrifugation procedure was repeated three times for purifying the Cu MOF products, which were subsequently dried under vacuum for 12 h at 60 °C. Finally, the obtained Cu MOFs were collected in 2 mL of deionized water for further use. Cu NCs were obtained by dropping 2 mL of 2 mM $NaBH_4$ into the above Cu MOF suspension and stirring for 2 h. After centrifugation and washing, Cu NCs were collected and stored in the dark.

### Electroanalysis of HTA or His using the Cu NC-modified electrodes

The optimization of the main electroanalysis conditions of the Cu NC-modified electrodes for sensing HTA and/or His was conducted using different amounts of Cu NCs (0.50, 1.0, 2.0, 4.0, and 6.0 mg $mL^{-1}$), pH values (1.0, 3.0, 5.0, 7.0, 9.0, 11, and 13), ionic strengths (20, 40, 60, 80, 100, 120, 140, 160, and 180 mM NaCl), and response times (10, 20, 30, 40, 50, and 60 s). Furthermore, the control tests were conducted accordingly with the Cu NC-modified electrodes separately for other kinds of ions and biological molecules (100.0 μM), including $Li^+$, $Na^+$, $K^+$, $Ag^+$, $NH_4^+$, $Ca^{2+}$, $Mg^{2+}$, $Zn^{2+}$, $Pb^{2+}$, $Cd^{2+}$, $Hg^{2+}$, $Al^{3+}$, $Cr^{3+}$, $Au^{3+}$, $S^{2-}$, His, Lys, Cys, Tyr, Gly, Ala, Phe, Glu, GSH, Tym, and DAB. In addition, the detection reproducibility for the HTA and/or His electroanalysis was evaluated using six Cu NC-modified electrodes.

Under the optimized conditions, the Cu NC-modified electrodes were applied for the electroanalysis of HTA and/or His with different concentrations in buffer. Typically, an aliquot of 2.5 μL Cu NC suspensions (2.0 mg $mL^{-1}$) optimized in 5.0% Nafion was dropped onto the glassy carbon electrodes for air drying. Square wave voltammetry (SWV) was performed at potentials ranging from −0.50 to 0.40 V at a scanning rate of 100 mV $s^{-1}$. Moreover, an aliquot of HTA and/or His with different concentrations (0–100.0 μM) was separately introduced into the phosphate buffer (pH 7.0, containing 100 mM NaCl) for the electrochemical SWV measurements. Subsequently, according to the same procedure, the developed electroanalysis method was employed for the evaluation of HTA and His with different concentrations spiked in red wine and urine samples, respectively. Herein, the red wine samples were prepared by following a modified method reported previously.[1] Briefly, an aliquot of 5.0 mL red wine and 5.0% trichloroacetic acid were added to centrifuge tubes followed by ultrasonic processing for 20 min. The supernatant was isolated by centrifugation and transferred to another tube. In the spike-in experiments, these samples with different HTA concentrations were pretreated by the above procedures. Besides, a baseline correction of the resulting voltammograms was conducted with the CHI software. The current changes refer to the differences of current responses between the Cu NC-modified electrodes before and after adding HTA and/or His of different concentrations.

It is noteworthy that all of the error bars represent the relative standard deviations (RSDs) of five quantitative results.

### Collection of urine samples

The urine samples were provided by the University Hospital at Qufu Normal University, and were collected from healthy volun-

 

teers with informed consent. All the experiments were performed in compliance with the Ethical Committee Approval of China, and approved by the ethics committee of Qufu Normal University.

## Results and discussion

### Synthesis and characterization of Cu NCs for HTA or His electroanalysis

Cu NCs were fabricated by using $NaBH_4$ to reduce Cu MOFs to be further modified onto the electrodes for the electroanalysis of HTA or His based on solid-state CuCl electrochemistry with "turn-on" signals, by which the background signals would be experimentally deducted. The main sensing principle and detection procedure are illustrated in Scheme 1, in which the Cu NC-modified electrodes display the electrochemical responses in turn to $Cl^-$ ions and then HTA or His, showing the rationally increasing CuCl oxidation currents. It is noteworthy that the $Cu^{2+}$ state in Cu MOFs might be reduced by $NaBH_4$ to yield the metallic $Cu^0$ state in Cu NCs,[39] which would be oxidized to the $Cu^+$ state on the Cu NC-modified electrodes during electrochemical scanning.[40] The resulting $Cu^+$ state would further interact with $Cl^-$ ions in solution to form non-conductive CuCl on the electrodes. Thus, the procedures of solid-state CuCl electrochemistry in the buffer containing $Cl^-$ ions are as follows:

$$Cu^0\ (solid) \rightarrow Cu^+\ (solid) + e^- \quad (1)$$

$$Cu^+\ (solid) + Cl^-(solution) \leftrightharpoons CuCl\ (solid) \quad (2)$$

$$CuCl\ (solid) + Cl^-(solution) \leftrightharpoons CuCl_2\ (solution) + e^- \quad (3)$$

$$CuCl_2\ (solution) + e^- \leftrightharpoons CuCl\ (solid) + Cl^-(solution) \quad (4)$$

In a whole repetitive electrochemical process, herein, the $Cu^0$ state in the Cu NCs modified on the electrodes could be electrochemically oxidized to the $Cu^+$ state, which would react with $Cl^-$ ions in solution to form CuCl solid on the electrodes. Moreover, the CuCl solid would be electrochemically oxidized to yield $CuCl_2$, which would be further reduced to CuCl in the reverse cathodic potential cycle. Furthermore, once HTA or His is introduced, it would convert CuCl into a Cu–HTA or His complex because of the stronger interaction between $Cu^{2+}$ and the imidazole groups of HTA or His. For example, the Cu–His interaction can form the product with the complexation constant of $K_{Cu-His} = 1.0 \times 10^{18.1}$.[41] As a result, the original non-conductive CuCl layers on the electrodes should be dissolved, so that the peaking oxidation currents of solid-state CuCl electrochemistry would increase,[30] which might also be evidenced by the various morphological structures of the corresponding products on the electrodes as revealed by their SEM images (top). A signal-"turn-on" electroanalysis strategy could be thereby expected for the analysis of HTA and/or His.

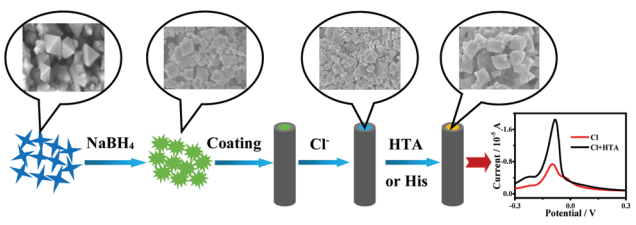


**Scheme 1** Schematic illustration of the preparation procedure of $NaBH_4$-treated Cu MOFs and electroanalytic sensing procedure with the step-by-step setup of the electrodes modified with Cu NCs for $Cl^-$ ions and then HTA with the electrochemical signal outputs, showing the corresponding SEM images of the resulting products (top).

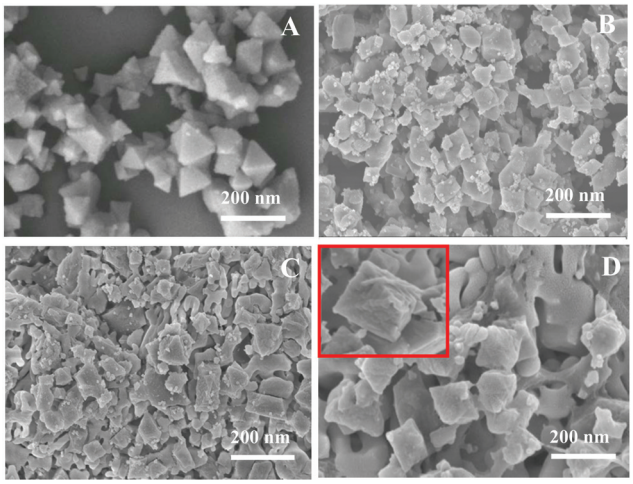


**Fig. 1** Characteristic SEM images of Cu MOFs (A) before and (B) after the treatment of $NaBH_4$ to yield Cu NCs; the Cu NCs after reacting first with (C) $Cl^-$ ions and then with (D) HTA.

Fig. 1 shows the detailed SEM images for Cu MOFs before and after being reduced by $NaBH_4$. As expected, the prepared Cu MOFs could display a well-defined octahedral structure (Fig. 1A). After the $NaBH_4$ reduction reactions, their structure could be collapsed with the surfaces full of some particle-like precipitates (Fig. 1B), in which the $Cu^{2+}$ state would be reduced into the metallic $Cu^0$ state. Moreover, the $Cu^0$ state would be electrochemically oxidized to yield the $Cu^+$ state, which would react with $Cl^-$ ions in solution resulting in increased blocky precipitates (Fig. 1C), which might be ascribed to CuCl precipitation through $Cl^-$–$Cu^+$ interactions on the Cu NCs of $NaBH_4$-treated Cu MOFs. When HTA was added further, to our surprise, the products would exhibit their smooth surfaces yet with a fluffy structure (Fig. 1D), as more clearly witnessed in the amplified view (insert), on which the blocky CuCl precipitates might be dissolved because of the strong Cu–HTA interactions. The data of SEM images apparently demonstrate the changing structures of $NaBH_4$-treated Cu MOFs during the interactions first with $Cl^-$ ions and then with HTA, thus promising the electroanalysis of HTA and/or His through the signal output of rationally increasing oxidation currents of solid-state CuCl electrochemistry.

### Electrochemical sensing properties of the Cu NC-modified electrodes

The Cu NC-modified electrodes were employed for the electroanalysis of HTA as an example through solid-state CuCl

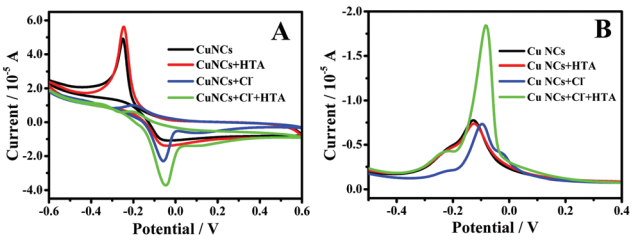


Fig. 2 Comparison of electrochemical (A) CV and (B) SWV responses of Cu NC-modified electrodes to blank (black), HTA (no $Cl^-$ ions, red), $Cl^-$ ions (blue), and then HTA (green) at a sweep rate of 100 mV $s^{-1}$.

electrochemistry (Fig. 2). Fig. 2A describes the responses of cyclic voltammetry (CV) of the developed electrodes when adding $Cl^-$ ions and then HTA in turn. It was noted that the as-prepared electrodes could display the reversible CV process of Cu redox peaks in the buffer without $Cl^-$ ions. A large Cu reduction peak could be obtained at a potential of about −0.25 V. Yet, when $Cl^-$ ions at high levels (*i.e.*, 100 mM) were introduced, the Cu NC-modified electrode could display the sharp oxidation peak of solid-state CuCl at about −0.10 V. More importantly, the current response to HTA in the presence of $Cl^-$ ions could be much larger than that in the absence of $Cl^-$ ions. Such a phenomenon could also be witnessed for the responses of square wave voltammetry (SWV) to HTA with and without the addition of $Cl^-$ ions (Fig. 2B). Notably, this low peak potential of CuCl electrochemistry (*i.e.*, −0.10 V) would aid in circumventing the possible interference from other electroactive substances in media especially those with the overlapped voltammetric signatures. What's more, a larger "turn-on" response to HTA could be expected for the Cu NC-modified electrodes with the signal output of solid-state CuCl electrochemistry, thus promising highly selective and sensitive HTA electroanalysis.

### Optimization of the electroanalysis conditions

The analysis conditions of the Cu NC-modified electrodes in sensing HTA as an example were optimized, mainly including the Cu NC dosages, pH values, $Cl^-$ (NaCl) concentrations, and response time (Fig. 3). The results indicate that the HTA-induced current changes can increase with increasing Cu NC dosages till 2.0 mg $mL^{-1}$, over which the signals would gradually decrease (Fig. 3A). This phenomenon might presumably be attributed to the fact that much denser Cu NC modifiers might be stacked onto the electrode surfaces, leading to the decrease in the conductivity. Accordingly, 2.0 mg $mL^{-1}$ of Cu NCs were thought to be the optimal amount in the experiments. Fig. 3B shows that pH values could influence the CuCl signals. Obviously, the highest peak currents of CuCl oxidation could be obtained at pH 7.0, which should be selected as the most suitable one. Meanwhile, as clearly disclosed in Fig. 3C, the peak currents could increase with the $Cl^-$ concentration increasing up to 100.0 mM, over which the currents could gradually decrease. Accordingly, 100.0 mM $Cl^-$ was chosen as optimal for sensing HTA. Fig. 3D exhibits the response time of

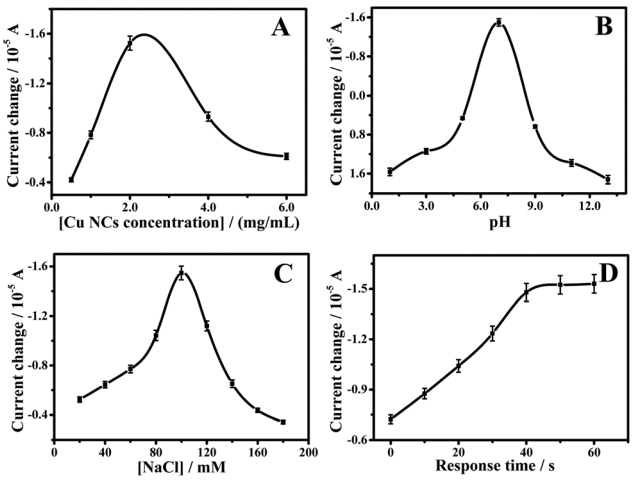


Fig. 3 Electrochemical HTA responses of Cu NC-modified electrodes depending on (A) the Cu NC concentrations, (B) different pH values (1.0–13), (C) ionic strengths at different NaCl concentrations (20–180 mM), and (D) response time in sensing HTA (100 μM).

the Cu NC-modified electrodes, revealing that the HTA response could be completed within 40 s.

### Investigations on the electroanalysis selectivity

The electroanalysis selectivity of the Cu NC-modified electrodes were explored for HTA or His, in comparison with that for some common ions and small molecules or amino acids, which may possibly co-exist in samples such as urine or red wine (Fig. 4). To our surprise, the other kinds of tested analytes alone could present the negligibly decreased responses, except for lysine (Lys) (Fig. 4A). Yet, Lys might display a noticeable response that is four times lower than that of HTA or His at the same concentration (Fig. 4A, inset). Also, the Cu NC-modified electrodes could measure HTA when separately mixed with these possibly interfering substances (Fig. 4B). Accordingly, the developed electroanalysis method can present high selectivity for probing HTA or His in some complicated samples such as urine or red wine. Moreover, electrochemical investigations were carried out on the storage stability of Cu NCs used in the HTA or His electroanalysis (Fig. 5A). As

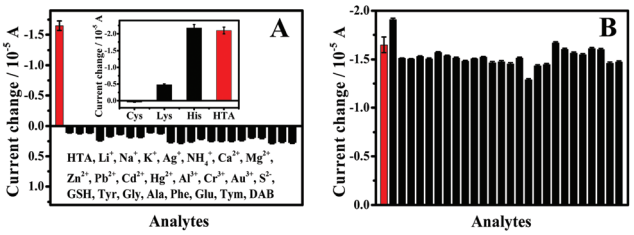


Fig. 4 Selective electrochemical responses of the Cu NC-modified electrode separately to (A) different interfering analytes indicated (inset: comparison of current changes among HTA, His, Lys, and Cys) (100.0 μM), and (B) those interfering analytes mixed separately with HTA with the same concentration.

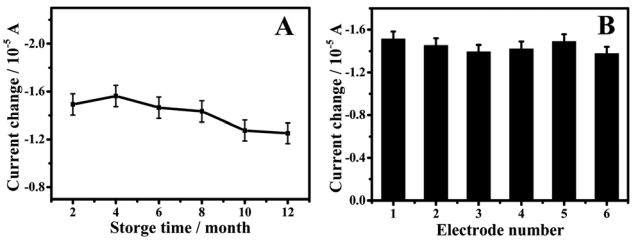


Fig. 5 (A) The storage stability of the prepared Cu NCs stored in the dark for different time intervals indicated before being modified onto the electrodes. (B) The electroanalysis reproducibility for sensing HTA (100 μM) using the Cu NC-modified electrodes.

expected, no significant change of HTA or His responses was monitored using the electrodes modified with Cu NCs that were stored even up to 12 months. Besides, the detection reproducibility of the developed electroanalysis was evaluated in sensing HTA or His, showing a statistic standard deviation of 4.2% for the results obtained using six Cu NC modified electrodes (Fig. 5B). The data indicate that the developed electrochemical HTA or His sensor could present pretty high detection selectivity and reproducibility, in addition to the long-term storage stability of Cu NCs.

### Electroanalysis of HTA or His in samples

Under the optimized conditions, the developed electroanalysis method with $NaBH_4$-treated Cu MOFs was applied for separately sensing HTA and His with different concentrations in buffer (Fig. 6). It was discovered that the current responses of the developed electrodes would increase with the increase in HTA concentrations (Fig. 6A). A linear relationship was thus obtained for the electrochemical responses *versus* the HTA concentrations ranging from 0.010 to 100 μM (Fig. 6B), with a limit of detection (LOD) of about 2.5 nM, estimated by the 3σ rule. Also, the electroanalysis of His was conducted showing basically the same linear range and LOD (Fig. 6C). Moreover, linear relationships were obtained for the electrochemical responses *versus* the concentrations of HTA mixed with His ([HTA/His]) in buffer ranging from 0.050 to 80 μM (Fig. 6D). In addition, the detection performances of the developed strategy for sensing HTA as an example were compared with those of the current detection methods reported previously, with the results summarized in Table S1.† One can note that the developed electroanalysis method can present better or comparable detection performances in terms of the detection ranges and LODs.

Subsequently, the application feasibility was investigated by employing the developed electroanalysis method to probe HTA and His separately in red wine and urine samples, both showing recoveries ranging from about 91 to 98.3% (Table S2†). The above results indicate that the developed electroanalysis platform with Cu NCs of $NaBH_4$-treated Cu MOFs can allow for the sensitive detection of HTA or His in complicated samples such as red wine and urine.

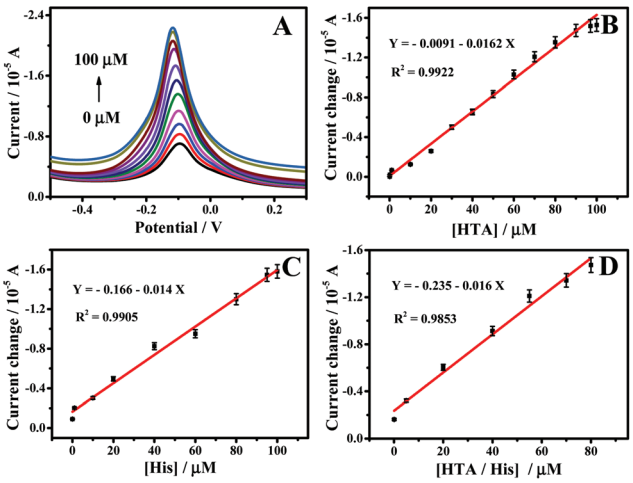


Fig. 6 (A) Electrochemical SWV responses to HTA of different concentrations in buffer measured at a sweep rate of 100 mV $s^{-1}$. The calibration curve for the relationship between the current responses and different concentrations of (B) HTA, (C) His, and (D) an HTA/His mixture in buffer.

## Conclusion

In summary, a highly selective and sensitive "turn-on" electroanalysis method has been successfully developed for sensing HTA and His separately in red wine and urine based on solid-state CuCl electrochemistry. The so-developed electroanalysis strategy can possess some outstanding advantages in comparison with the current analysis methods for sensing HTA or His. First, the Cu NC-modified electrodes could present responses to HTA and His with the "turn-on" signal outputs, which may help achieve highly selective detection of HTA and His in complicated media. Second, solid-state CuCl electrochemistry can ensure sharp and large current responses to HTA or His at a considerably low potential (*i.e.*, −0.10 V), so as to avoid the interference from electroactive substances possibly co-existing in the sample backgrounds. Third, high detection reproducibility can be expected for sensing HTA and His by using Cu NCs of $NaBH_4$-treated Cu MOFs with long-term stability. Finally, this electrochemical sensor can allow for the highly selective and sensitive evaluation of HTA and His separately in complicated red wine and urine samples, and its analysis performances can be better or comparable to those of the detection methods previously reported. Therefore, such an electroanalysis method can be promising for practical applications in the evaluation of HTA or His at trace levels in complicated media for food analysis and the early warning or diagnosis of some serious diseases.

## Conflicts of interest

There are no conflicts to declare.

## Acknowledgements

This work is supported by the National Natural Science Foundations of China (No. 21675099); the Major Basic Research Program of Natural Science Foundation of Shandong Province (ZR2018ZC0129), and the Key R&D Plan of Jining City (2018HMNS001), Shandong, P. R. China.

## Notes and references

1 A. Han, L. Xiong, S. Hao, Y. Yang, X. Li, G. Fang, J. Liu, Y. Pei and S. Wang, *Anal. Chem.*, 2018, **90**, 9060–9067.
2 P. Q. Leng, F. L. Zhao, B. C. Yin and B. C. Ye, *Chem. Commun.*, 2015, **51**, 8712–8714.
3 M. Peeters, F. J. Troost, R. H. Mingels, T. Welsch, B. van Grinsven, T. Vranken, S. Ingebrandt, R. Thoelen, T. J. Cleij and P. Wagner, *Anal. Chem.*, 2013, **85**, 1475–1483.
4 D. Nei, N. Nakamura, K. Ishihara, M. Kimura and M. Satomi, *Food Control*, 2017, **75**, 181–186.
5 J. Sun, Z. Qin, J. Liu, C. Zhang and H. Luo, *Analyst*, 2014, **139**, 3154–3159.
6 S. Khan, L. S. A. Carneiro, M. S. Vianna, E. C. Romani and R. Q. Aucelio, *J. Lumin.*, 2017, **182**, 71–78.
7 L. Luo, J. Y. Yang, Z. L. Xiao, D. P. Zeng, Y. J. Li, Y. D. Shen, Y. M. Sun, H. T. Lei, H. Wang and Z. L. Xu, *RSC Adv.*, 2015, **5**, 78833–78840.
8 S. Jiang, Y. Peng, B. Ning, J. Bai, Y. Liu, N. Zhang and Z. Gao, *Sens. Actuators, B*, 2015, **221**, 15–21.
9 M. Akhoundian, A. Ruter and S. Shinde, *Sensors*, 2017, **17**, 645–654.
10 X. Zheng, T. Yao, Y. Zhu and S. Shi, *Biosens. Bioelectron.*, 2015, **66**, 103–108.
11 L. D. Pettit and J. L. M. Swash, *Cheminform*, 1976, **7**, 588–594.
12 L. Zhou, S. Li, Y. Su, X. Yi, A. Zheng and F. Deng, *J. Phys. Chem. B*, 2013, **117**, 8954–8965.
13 Y. Hu, Q. Wang, C. Zheng, L. Wu, X. Hou and Y. Lv, *Anal. Chem.*, 2014, **86**, 842–848.
14 S. K. Sun, K. X. Tu and X. P. Yan, *Analyst*, 2012, **137**, 2124–2128.
15 S. Qiu, M. Miao, T. Wang, Z. Lin, L. Guo, B. Qiu and G. Chen, *Biosens. Bioelectron.*, 2013, **42**, 332–336.
16 J. T. Hou, K. Li, K. K. Yu, M. Y. Wu and X. Q. Yu, *Org. Biomol. Chem.*, 2013, **11**, 717–720.
17 M. Maldonado and K. Maeyama, *Anal. Biochem.*, 2013, **432**, 1–7.
18 G. Duflos, G. Inglebert, C. Himber, S. Degremont, B. Lombard and A. Brisabois, *Int. J. Food Microbiol.*, 2019, **288**, 97–101.
19 S. Köse, N. Kaklıkkaya, S. Koral, B. Tufan, K. C. Buruk and F. Aydın, *Food Chem.*, 2011, **125**, 1490–1497.
20 J. Cai, M. Li, X. Xiong, X. Fang and R. Xu, *J. Mass Spectrom.*, 2014, **49**, 9–12.
21 W. Liaoa, H. Paekb, C. Mabunia, S. Angoldb and M. Solimana, *J. Chromatogr., A*, 1999, **853**, 541–544.
22 M. Hashemi, Z. Nazari and N. Noshirvani, *Carbohydr. Polym.*, 2017, **177**, 306–314.
23 T. Kuda, T. Mihara and T. Yano, *Food Control*, 2007, **18**, 677–681.
24 X. Feng, J. Ashley, T. Zhou, A. Halder and Y. Sun, *RSC Adv.*, 2018, **8**, 2365–2372.
25 N. Kumar and R. N. Goyal, *Sens. Actuators, B*, 2018, **268**, 383–391.
26 M. Liu, L. Zhang, Y. Hua, L. Feng, Y. Jiang, X. Ding, W. Qi and H. Wang, *Anal. Chem.*, 2017, **89**, 9552–9558.
27 R. Li, S. Li, M. Dong, L. Zhang, Y. Qiao, Y. Jiang, W. Qi and H. Wang, *Chem. Commun.*, 2015, **51**, 16131–16134.
28 X. X. Dong, J. Y. Yang, L. Luo, Y. F. Zhang, C. Mao, Y. M. Sun, H. T. Lei, Y. D. Shen, R. C. Beier and Z. L. Xu, *Biosens. Bioelectron.*, 2017, **98**, 305–309.
29 R. K. R. Gajjala and S. K. Palathedath, *Biosens. Bioelectron.*, 2018, **102**, 242–246.
30 Y. T. Lin, C. H. Chen and M. S. Lin, *Sens. Actuators, B*, 2018, **255**, 2838–2843.
31 U. T. Yilmaz and D. Inan, *J. Food Sci. Technol.*, 2015, **52**, 6671–6678.
32 J. Zhang, B. P. Ting, N. R. Jana, Z. Gao and J. Y. Ying, *Small*, 2009, **5**, 1414–1417.
33 Y. Zhao, L. Xu, S. Li, Q. Chen, D. Yang, L. Chen and H. Wang, *Analyst*, 2015, **140**, 1832–1836.
34 Y. Hua, X. Lv, Y. Cai, H. Liu, S. Li, Y. Wan and H. Wang, *Chem. Commun.*, 2019, **55**, 1271–1274.
35 C. Fan, X. Lv, F. Liu, L. Feng, M. Liu, Y. Cai, H. Liu, J. Wang, Y. Yang and H. Wang, *ACS Sens.*, 2018, **3**, 441–450.
36 R. B. Lin, F. Li, S. Y. Liu, X. L. Qi, J. P. Zhang and X. M. Chen, *Angew. Chem., Int. Ed.*, 2013, **52**, 13429–13433.
37 L. Ji, Q. Cheng, K. Wu and X. Yang, *Sens. Actuators, B*, 2016, **231**, 12–17.
38 W. J. Shen, Y. Zhuo, Y. Q. Chai and R. Yuan, *Anal. Chem.*, 2015, **87**, 11345–11352.
39 D. Song, J. Bae, H. Ji, M.-B. Kim, Y.-S. Bae, K. S. Park, D. Moon and N. C. Jeong, *J. Am. Chem. Soc.*, 2019, **141**, 7853–7864.
40 Y. Si, Z. Sun, N. Zhang, W. Qi, S. Li, L. Chen and H. Wang, *Anal. Chem.*, 2014, **86**, 10406–10414.
41 J. F. Folmer-Andersen, V. M. Lynch and E. V. Anslyn, *Chemistry*, 2005, **11**, 5319–5326.